Preprint, 15th Conf. on Numerical Weather Prediction and 19th Conf. on Weather Analysis and Forecasting

2.1 SENSITIVITY OF MODEL THUNDERSTORMS TO MODIFICATIONS TO THE ENIRONMENTAL CONDITIONS BY A NEARBY THUNDERSTORM IN THE PREDICTION OF 2000 FORT WORTH TORNADO CASE

Ming Hu and Ming Xue
School of Meteorology and Center for Analysis and Prediction of Storms
University of Oklahoma, Norman, OK 73019

1. INTRODUCTION

It is generally recognized that the environmental buoyancy and vertical wind shear have important effect on the characteristics of convective storms. Parameters and indices, such as the bulk Richardson number (BRN) and environmental storm-relative helicity, have been commonly used in both research and operations to characterize the environmental properties important to thunderstorm development and evolution. Much of our understanding of the sensitivity of convective storms to these environment parameters has been derived from modeling studies that tested a varieties of, but often idealized, environmental conditions (e.g., Weisman and Klemp 1984, 1982; Eugene and Morris 2001). The real-world buoyancy and wind profiles are, however, often much more complex than can be adequately described by a few simple parameters. In fact, we found, through the study of a model-predicted real convective system, that a very small change in the mid-to-low level wind profile can produce very different behaviors of storms after their splitting.

The case studied is that of the 2000 Fort Worth tornado. In this case, the initial development and evolution of the thunderstorm that spawned that Fort Worth tornado was well simulated. However, this storm's evolution deviated from reality in the hour following the tornado outbreak due to its merging with a cell that was a spuriously intensified left mover from another storm to its front right. In reality, this left-mover dissipated quickly after initial splitting. This paper attempts to identify the cause of this incorrect behavior and in the process investigates the sensitivity of thunderstorms to small changes in the environmental conditions.

2. FORT WORTH TORNADO CASE

An F2 tornado struck downtown Fort Worth, TX, at around 0020UTC, March 29, 2000 (6:20pm LST March 28). The tornado stayed on the ground for at least 15 minutes, creating a path of about 3 mile long with severe damages to buildings in the downtown area.

The high-resolution numerical simulations of this case were rather successful in predicting more than 1 hour ahead of time the timing and location of a tornadic supercell storm (referred to as the tornadic storm hereafter) over Fort Worth. The model-predicted low-level rotation center was within kilometers from downtown Fort Worth at the time of tornado touchdown (Xue *et al.* 2001; Wang *et al.* 2001). The numerical model used was the Advanced Regional Prediction System (ARPS) of CAPS, University of Oklahoma (Xue *et al.* 2000).

Corresponding author address: Ming Xue, SOM, U. of Oklahoma, Norman OK 73019. E-mail: mxue@ou.edu.

The 1-hour model predicted low-level reflectivity fields and the corresponding radar observations are shown in Fig. 1. Comparing Fig. 1b with 1d, we can see that storm cell A in the model deviated from the observed one by 1.5 hours and even more later on (not shown). Comparison of the 1 hour forecast (Fig. 1a) and the corresponding radar observation (Fig. 1c) shows that a spurious cell B′ is found to the southeast of cell A. This spurious cell moved north-northeastward and by 1.5 hours it has merged with cell A (Fig. 1d). Further investigation showed that cell B′ was the overly intensified left mover of storm B (Fig.1c) that split during the first forecast hour. In reality, the left-mover did not fully develop into a mature cell while the right mover (storm B in Fig. 1) dominated all the time.

3. IDEALIZED SIMULATION EXPERIMENTS USING MODEL EXTRACTED SOUNDINGS

In order to understand why the splitting storm B behaved the way it did in the model, we examined the environment surrounding this storm. Vertical sounding profiles were extracted from locations X, Y and Z shown in Fig. 2 at times proceeding or near the time of splitting. To examine the impact of environment on model simulated storms, a series of idealized simulations are performed, in which storms were initialized by a thermal bubble in horizontally homogeneous environments defined using the extracted soundings.

3.1 Experimental design

First, we reran the 3-km simulation reported in Xue et al (2002) using a 1-km resolution, starting from the initial condition interpolated from the 3-km assimilated fields at 23 UTC. The grid size was 450x300x43 and the vertical grid is stretched from 20 m at the ground level to close to 1 km at the 20 km high model top. The evolution of storms inside the model domain was generally similar to those in the 3 km domain, except that storm structures were more detailed. This suggests that the relatively coarse 3 km resolution was not the cause of the misbehavior. Figure 2 shows the composite reflectivity field at the initial time of 2300UTC 28 March 2000. The bold arrow in the figure starts from the location of storm B at this time and points in the direction that the left-moving cell B' propagated. Five soundings were extracts, three at 23:00 UTC, from locations marked as X, Y and Z in Fig. 2, and the other two at 23:15 and 23:30 UTC from location Z. The soundings extracted from X and Y represent the environment close to the storm at the beginning of splitting and those extracted from location Z, especially those at later times, represent the environment into which the left-mover propagated into.

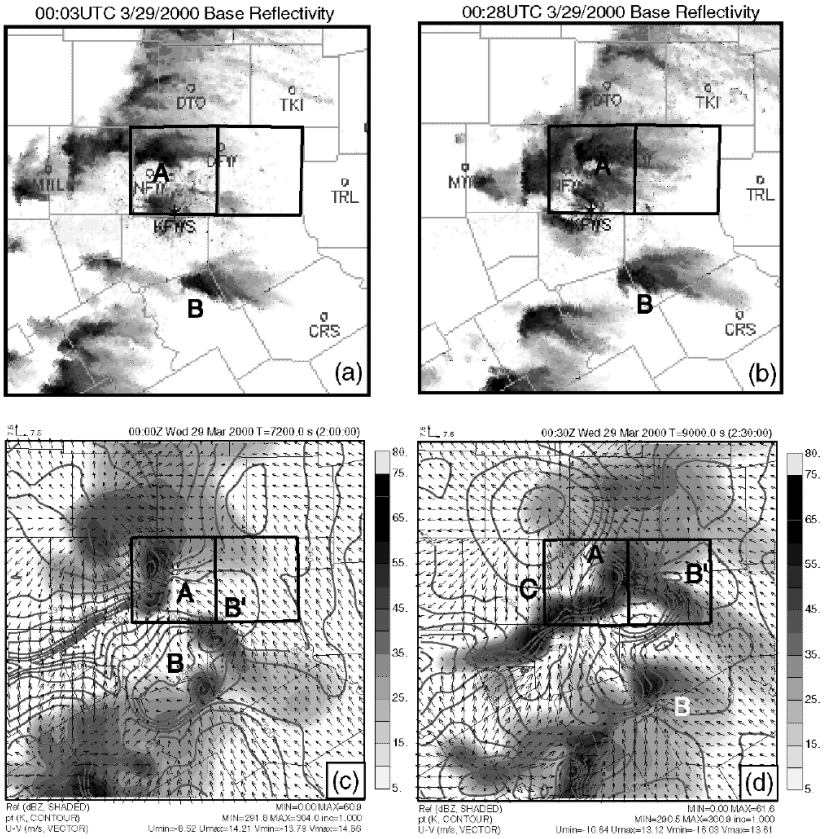

Fig. 1. Observed low-level radar reflectivity fields at 00:03UTC(a) and 00:28UTC(b), March 29, 2000 and the corresponding ARPS predicted fields valid at about the same times (c and d). Major storm cells are marked by capital letters A, B, B' and C. Forth Worth and Dallas are located near the center of highlighted Tarrant (left) and Dallas (right) counties, respectively.

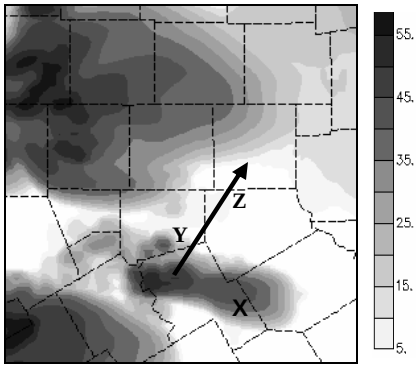

Fig. 2. Composite reflectivity field at initial time (2300UTC 28 March 2000) of real data simulation. The X, Y, and Z are the locations at which background soundings were extracted. The arrow indicates the path and direction of the left mover of split storm in the real-data simulation

Using the same horizontal (1 km) and vertical grid resolutions as our real data simulation, and similar physics as the real data run, we initialized convective storms in horizontally homogeneous environments using a single thermal bubble, and performed simulations for 2 hours. The experiments are listed in Table 1. Figure 3 shows the hodographs of the soundings used in experiments Z30 and Z30M. The hodograph in Z30M is the same as that of Z30, except that the v velocity below 6 km was modified so as to remove a slight counter-clockwise curvature seen in Z30. Overall, the hodograph curvatures are clockwise.

Table 1: Summary of experiments

Exp. Name	Characteristics of sounding used in experiment			
	Location	Time (UTC)	CAPE(J /kg)	Shear/6km (ms^{-1})
X00	X	23:00	3098	18.9
Y00	Y	23:00	2829	30.8
XY00	X+Y	23:00	3098	30.8
Z00	Z	23:00	2423	24.9
Z15	Z	23:15	2644	30.5
Z30	Z	23:30	2365	40.4
Z30M	Z	23:30	2365	40.4

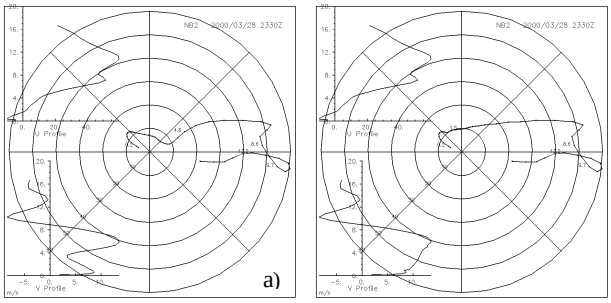

Fig. 3. Hodographs of soundings used in Z30(a) and Z30M(b)

3.2 The impact of the environmental conditions on storm evolution

Figure 4 shows the composite reflectivity fields at 1.5 hours of the idealized simulations, for experiments X00, Y00 and XY00 (c.f., Table 1). In X00 (Fig. 4a), three reflectivity maxima are visible but remain clustered together, in essence, the classic cell splitting did not occur in this case.

In Y00, only one storm cell is present at this time (Fig. 4b). Examination of earlier fields show that the original storm did split into two distinct cells during first hour but left cell persisted for a short time and then dissipated. From Table 1, we can see that X00 has larger CAPE but weaker vertical wind shear than Y00. This is consistent with our understanding that vertical wind shear promotes storm splitting (Klemp 1987).

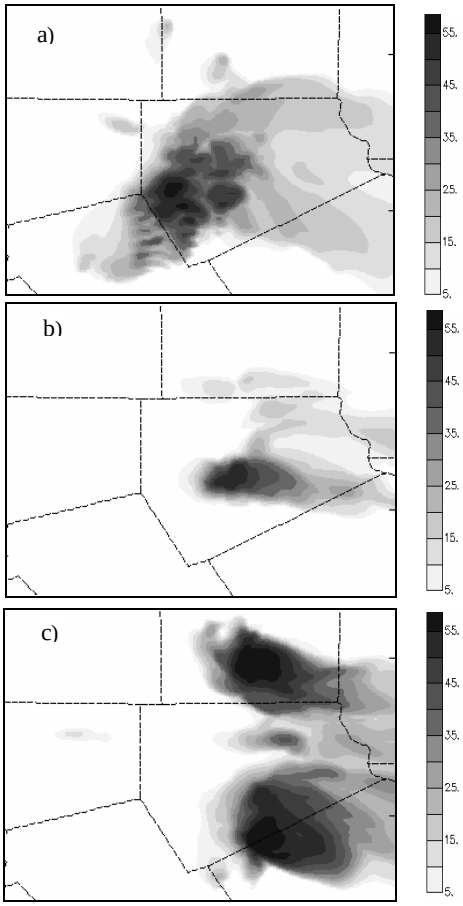

Fig. 4. Composite reflectivity fields from X00 (a), Y00 (b) and XY00(c), at 1.5 hours of simulation, roughly corresponding to 00:30UTC, 29 March 2000 of real time.

To understand the relative roles of thermal and wind profiles in producing the storm behaviors seen above, we performed experiment XY00 which used the temperature and moisture sounding profiles of X00 but wind profile of Y00. The results are very interesting. In this case, the storm split into two distinct cells of almost equal strength and both were stronger than their counterparts in X00 and Y00. Compared to Y00, apparently, a slight increase in the CAPE value (from a slight increase in the CAPE value (from 2829 to 3098 J kg^{-1} which is less than 10%) was enough to completely alter the behavior of the split cells. In this case, the mid-to-low level shear was strong enough to promote storm splitting while the CAPE was larger (though not much larger) than that of Y00 to sustain both split cells. The above results show a tremendous sensitivity of the simulated storms to the environmental shear and more so to convective stability.

The storm evolution of in Y00 is most close to the observed storm B shown in Fig.1, suggesting that, among the three, the environment of Y00 is probably most close to the real one. From Fig. 2, we can see that the environment represented by Y00 is the one in which the storm began to split and further develop. The reason why storm B (c.f., Fig.1) in the real data simulation did not develop like the one in experiment Y00 is, we believe, that the environment the actual split cell propagated into had changed significantly from that at 23UTC at location Y. In the following, soundings from more representative location Z, at the current time and at 15 and 30 min later, are examined. These experiments are denoted Z00, Z15 and Z30. An additional experiment, Z30M, used a wind profile modified from that of Z30 (c.f., Table 1).

The composite reflectivity fields from these four experiments at 1.5 hours are shown in Figure 5. The initial evolution of the storm cells in Z00 was similar to that of Y00, that is, the original storm split and its right mover dominated. By 1.5 hours, the left mover remained, however (Fig. 5a), while that in Y00 disappeared by this time despite significantly larger CAPE. The mid-to-low level shear in Y00 was stronger, which must have played a more dominant role than CAPE. Fifteen minutes later, both CAPE and shear increased at location Z, more in the latter. Both cells are stronger (Fig. 5b) than those in Z00, especially the right one. In 15 more minutes, the CAPE at location Z decreased from 2644 to 2365 J kg^{-1}, while the mid-to-low level shear further strengthened. Such changes completely altered the behavior of the split cells, making the left mover stronger. As seen from Fig. 5c, the right mover at 1.5 hours was rather weak. In the real data simulation, the left mover (B' in Fig. 1c) was slightly stronger therefore the storm behaviors were close to those of Z30. Since point Z is located in the region the left mover in the real data simulation moved into in the hour following the initial time, the profiles at Z30 represent the environment experienced by the split cell B' in the real data case. By examining these profiles, clues can be found as to why the left mover sustained its strength rather than dissipated as in reality.

We know from the theories of thunderstorms that hodographs with counterclockwise curvatures favor the left mover (Klemp 1987). In the hodograph of Z30 (Fig. 3a), we only found a small segment that has a counterclockwise curvature, and this segment is between the 1.5 and 4.5 km levels and the maximum curvature was at 3.2 km. To determine if this counterclockwise curvature indeed caused the left mover to become dominant, we modified the profile of v in Z30 to eliminate the counterclockwise segment and conducted simulation Z30 again with everything else remaining the same (Z30M). Sure enough, the storm behavior is changed – the right instead of left mover becomes dominant! The storm behavior of this run is similar to that of Z15. To further examine the relatively role of thermodynamic sounding versus wind shear, we completed three

more experiments in which the thermodynamic profiles of Z00, Z30 and Z30M were replaced with that of Z15. The resulting behaviors of storms were not much different from their counterparts shown in Fig. 5, suggesting that the thermodynamic profiles played only a secondary role in these cases while the wind profiles had the dominant control.

Careful analysis of the evolution of wind field at point Z shows that the west-southwest wind at the mid-to-low levels at point Z increased dramatically during this period because of the approaching of the tornadic storm from northwest (storm A in Fig. 1a). In Table 1, we see that the wind speed at 6km AGL increased by 10ms^{-1} in a 15 minute period (from Z15 to Z30). Such a wind change was responsible for the increase in the anticlockwise hodograph curvature at the mid-to-low levels, and therefore for the creation of an incorrect environment that favored the left mover.

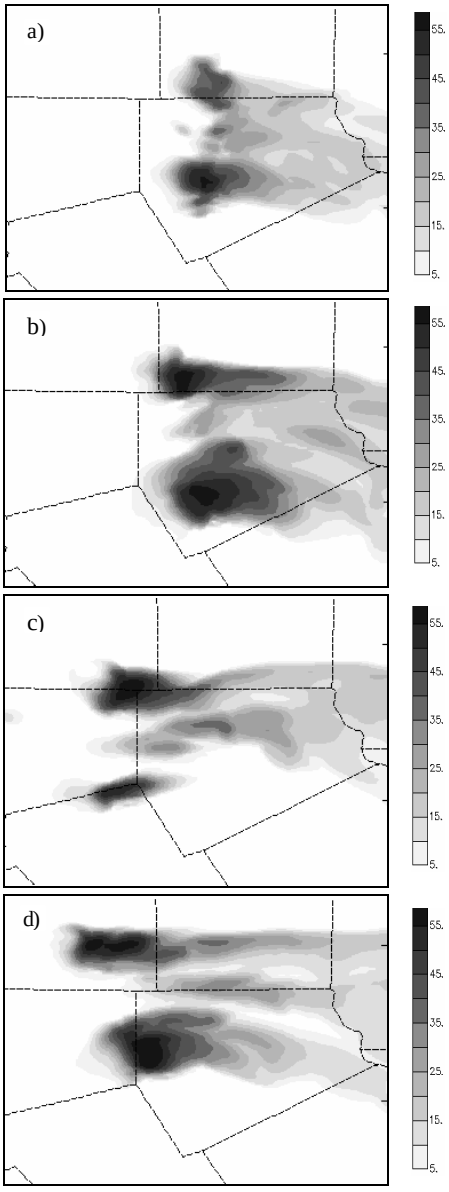

Fig. 5. Composite reflectivity fields at 1.5 hours of idealized simulations Z00 (a), Z15 (b), Z30 (c), and Z30M (d).

4. DISCUSSION

From the above experiments, we found that the model-simulated storms are very sensitive to seemingly small changes in the environmental wind profiles. A small counterclockwise curvature found in the hodograph at the mid-lower troposphere was all it took for the left-mover to become dominant. Because most of the wind speed change occurred below the 6 km level, standard lower troposphere Bulk Richardson number (BRN) or storm-relative environmental helicity would not work well as the predictors of storm characteristics, in fact, we will find no difference in BRN between Z30 and Z30M because the CAPE and wind shear from ground to 6 km are the same. The actual storms behaved very differently in these two experiments. In the above, especially in the second series of experiments, the model storms were not very sensitive to small differences in the thermodynamic profiles.

Our idealized numerical experiments revealed clearly that the incorrect behaviors of the splitting storm in the real data case were mainly caused by the presence of a shallow layer of counterclockwise curvature in the lower tropospheric wind profile. Evidences exist that show that this counterclockwise curvature was induced by the approaching tornadic thunderstorm. This small counterclockwise curvature was responsible for the spurious intensification of the left-moving storm that subsequently interfered with the tornadic thunderstorm in the post-tornadic phase. The results also illustrate a way by which two nearby thunderstorm interact indirectly but effectively by modifying each other's environment. The sensitivity we have seen here has important implications to the forecast of such storm systems. Our future work will involve the assimilation of radial velocity data from the Fort Worth radar, with the goal of correcting the mid-level winds for better predictions of storm B and the later evolution of the tornadic storm A.

References

Eugene, W. M. and L. W. Morris, 2001: The sensitivity of simulated supercell structure and intensity to variations in the shapes of environmental buoyancy and shear profiles. *Mon. Wea. Rev.*, **129,** 664-686.

Klemp, J. B., 1987: Dynamics of tornadic thunderstorms. *Annul Rev. Fluid. Mech.*, **19,** 369-402.

Wang, D., K. K. Droegemeier, D. Jahn, K.-M. Xu, M. Xue, and J. Zhang, 2001: NIDS-based intermittent diabatic assimilation and application to storm-scale numerical weather prediction. *Preprint, 14th Conf. on Num. Wea. Pred.*, Ft. Lauderdale, Florida, Amer. Met. Soc.

Weisman, M. L. and J. B. Klemp, 1982: The dependence of numerically simulated convective storms on vertical wind shear and buoyancy. *Mon. Wea. Rev.*, **110,** 504-520.

Weisman, M. L. and J. B. Klemp, 1984: The structure and classification of numerically simulated convective storms in directionally varying wind shears. *Mon. Wea. Rev.*, **112,** 2479-2498.

Xue, M., K. K. Droegemeier, and V. Wong, 2000: The Advanced Regional Prediction System (ARPS) - A multi-scale nonhydrostatic atmospheric simulation and prediction model. Part I: Model dynamics and verification. *Meteor. Atmos. Phys.*, **75,** 161.

Xue, M., D.-H. Wang, J.-D. Gao, K. Brewster, and K. K. Droegemeier, 2001: The Advanced Regional Prediction System (ARPS), storm-scale numerical weather prediction and data assimilation. *Meteor. Atmos. Physics***,** In press.